Study of Adsorption Kinetics of Perfluoroisobutene on Fixed Bed Activated Carbon

Pingwei Ye,[†,‡] Zhiqiang Luan,[‡] Jingchang Zhang,*[,†] Zhongliang Zhang,[†] Lan Ma,[‡] Kai Li,[‡] Lei Li,[‡] Yan Li,[‡] and Weiliang Cao[†]

Beijing University of Chemical Technology, Beijing 100029, China, and Research Institute of Chemical Defense, Beijing 100083, China

The adsorption dynamics of perfluoroisobutene (PFIB) on fixed bed activated carbon under various humidity conditions was studied, and the granular activated carbon was treated using a microwave. The equilibrium adsorption capacities and adsorption rate constants were calculated using the Wheeler equation. The dynamic model based on linear equilibrium was used to correlate the entire experimental data, and the theoretical breakthrough curves of PFIB on the carbon bed were then obtained. The results showed that the pore structure did not change obviously, but the surface oxygen content decreased after microwave modification. The selective adsorption capacities to PFIB increased greatly, and the carbon bed's effective protection time against PFIB was prolonged under high airflow humidity. The theoretical breakthrough curves agreed with the experimental data very well, and this kinetic model can be used to predict the breakthrough behavior and to design and select the parameters of the respirator cartridges.

Introduction

Activated carbon is widely used to remove pollutants from air in respirator cartridges.[1] Efficiencies and service lives of such carbon beds need to be known for application, design, and maintenance decisions.[2] There are many parameters which influence an adsorption process and thus affect the performance of the activated carbon, e.g., properties and concentration of contaminants in air, properties of the carbon bed, atmospheric conditions (temperature and relative humidity), and flow rate of air.[1]

Perfluoroisobutene, commonly known as PFIB, is a colorless, highly toxic gas, approximately 10 times as toxic to the lungs as phosgene.[3] It is generated from thermal decomposition of polytetrafluoroethylene (e.g., Teflon) and other perfluoropolymers.[4] Overheating of insulating material generates fumes that may pose a serious health hazard to the respiratory tract in humans, resulting in so-called "polymer fume fever" with symptoms ranging from slight irritation to severe pulmonary edema.[5] The activated carbon respirator cartridges are usually used for the protection of PFIB contaminated air. The molecular structure of PFIB is symmetrical and nonpolar, so it is hard to adsorb by common activated carbon. Many investigators have studied the adsorptive kinetics of activated carbon against many pollutants,[6–10] but there are very few reports about the breakthrough behavior of PFIB on a bed of activated carbon.

According to the practical requirement of respirator cartridges, in this paper, the breakthrough behavior of PFIB on untreated and microwave modified carbon beds at various humidity conditions was investigated.

* Corresponding author. E-mail: zhangJC1@mail.buct.edu.cn. Tel.: 086-010-64434904.
† Beijing University of Chemical Technology.
‡ Research Institute of Chemical Defense, Beijing.

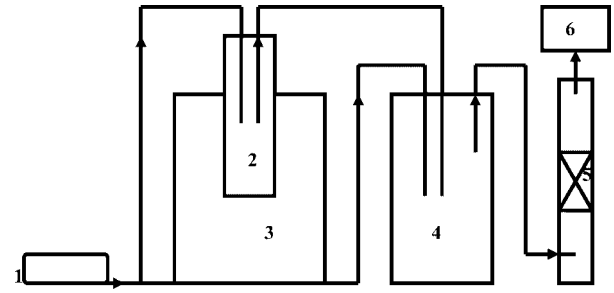

Figure 1. Schematic of experimental setup for the adsorption process: 1, air compressor; 2, gas generator of PFIB; 3, thermostatic bath; 4, gas mixer; 5, activated carbon bed; 6, gas chromatography.

Experimental Section

Materials and Analysis. The activated carbon used in the experiments was Φ 0.9 mm × 5 mm. The N_2 adsorption isotherms were tested with an Autosorb1-type adsorption instrument produced by Quantachrome Company. The surface oxygen content was analyzed by an XPS analyzer (XSAM-800, Kratos, Co., Britain). The vapor penetration of the bed was detected by gas chromatography (HP6890).

Experimental Process. (a) Microwave Modification. The activated carbons were put into a quartz tube which was fixed in a microwave apparatus. The power of the microwave was 800 W, and the treated time of samples in N_2 flow was (60, 120, and 180) s, respectively. The treated samples were named as M-60, M-120, and M-180.

(b) Adsorption Apparatus. The adsorption kinetic tests were carried out with a vapor adsorption test apparatus. The apparatus, shown in Figure 1, includes a gas generator of PFIB, a thermostatic bath, an adsorption column, and the gas chromatography for the detection of PFIB vapor.

(c) Procedure. The granule activated carbons used in the tests were dried at 120 °C for at least 4 h prior to the adsorption tests and packed in the cylindrical stainless steel sample holder.

10.1021/je7006346 CCC: $40.75 © 2008 American Chemical Society
Published on Web 05/10/2008

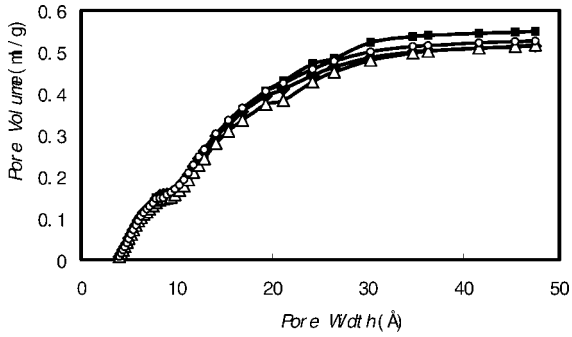

Figure 2. DFT cumulative pore volume plot: ◆, untreated; ■, H-60; △, H-120; ○, H-180.

Table 1. Effect of Microwave Modification on the Specific Area and Pore Structure

sample	S_{BET} $m^2 \cdot g^{-1}$	micropore volume $mL \cdot g^{-1}$	mesopore volume $mL \cdot g^{-1}$
untreated	1237	0.5401	0.0921
H-60	1263	0.5494	0.1059
H-120	1255	0.5444	0.0962
H-180	1275	0.5477	0.0991

Table 2. Oxygen Contents of Samples Before and After Modification

sample	untreated	M-60	M-120	M-180
oxygen content (%)	5.37	3.24	2.90	2.74

The airflow rate was calibrated by mass flow meters. The high concentration air flow was mixed with another air in the gas mixer to obtain a gas stream with a given concentration and was then directed into the activated carbon bed with a constant flow velocity. The adsorption bed was Φ 20 mm × 20 mm; the concentration of the inlet PFIB−air mixture was 4 $mg \cdot L^{-1}$; and the gas flow rate was 0.25 $L \cdot min^{-1} \cdot cm^{-2}$. The tests were carried out at 30 %, 40 %, 50 %, 60 %, and 80 % airflow humidity.

Results and Discussion

Effect of Microwave Modification on S_{BET} and Pore Structure. The specific area of test samples was calculated from the BET method, micropore volume from the MP method, and mesopore volume from the BJH method. The pore structures of the samples before and after microwave treatment are listed in Table 1. After microwave modifications, the S_{BET}, micropore volume, and mesopore volume and the pore volume distributions of the four samples calculated by the DFT (Density Functional Theory) method in Figure 2 did not change obviously.

Effect of Microwave Treatment on Surface Oxygen Content. The surface oxygen of the samples before and after modification was analyzed by an XPS analyzer. As shown in Table 2, the surface oxygen of the untreated carbon is 5.37 %, and that of the M-180 is 2.74 %, indicating that a large fraction of the oxygen-containing groups was removed from the carbon surface.

Breakthrough Process. (a) Breakthrough Curves. As shown in Figure 3, each curve is "S" shaped, and the higher the airflow humidity, the shorter the protection time of the carbon bed against PFIB. The reason is that water molecules adsorb competitively with the PFIB molecules. The competition effect became greater with the increase of the humidity of airflow.

(b) Results of Data Processed with the Wheeler Equation (Low Concentration Penetration Equation). The Wheeler adsorption kinetics equation, initially derived from the equation

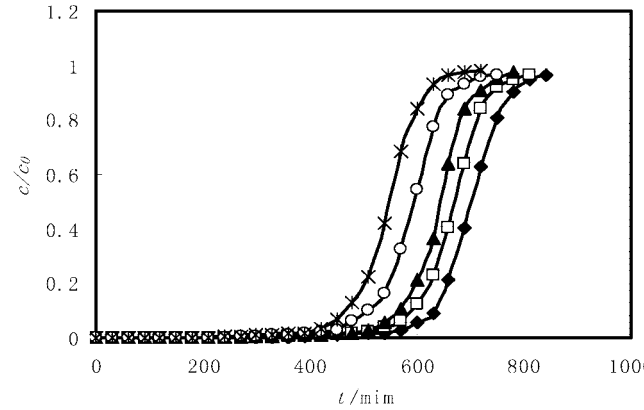

Figure 3. Breakthrough curves at different flow humidity conditions for untreated carbon: ◆, 30 %; □, 40 %; ▲, 50 %; ○, 60 %; ×, 80 %. (E-Experimental; T-Theoretical; Inlet concentration, 4 $mg \cdot L^{-1}$; experiment temperature, 25 °C.)

of mass balance between the gas entering an adsorbent bed and the sum of the gas adsorbed plus that penetrating through the bed, can be shown in the polynomial form[11]

$$t_b = \frac{q_e}{c_0 v}\left[L - \frac{v \cdot 10^3}{k_v} \ln(c_0/c_x)\right] \quad (1)$$

In eq 1, t_b is the gas breakthrough time in min; c_0 is the inlet concentration in $mg \cdot L^{-1}$; v is the flow rate in $L \cdot min^{-1} \cdot cm^{-2}$; L is the bed length in cm; k_v is the adsorption rate constant in min^{-1}; q_e is the equilibrium adsorption capacity in $mg \cdot cm^{-3}$.

The Wheeler equation is only suitable for low concentration penetration, not for the entire breakthrough curve, so it is also commonly known as the low concentration penetration equation.

Based on the low concentration penetration points of the breakthrough curve, a regression plot of t_b $\ln(c_0/c_x)$, for any fixed flow rate and temperature, was calculated. The parameters q_e and k_v can be calculated from the slope and intercept of the regression equation, respectively. Figure 2 is the t_b $\ln(c_0/c_x)$ plot under various airflow humidity conditions. Generally, in the use of a respirator cartridge, the breakthrough time is denoted as the time when the exit stream shows the presence of a gas concentration equal to an exit to inlet concentration ratio (c_x/c_0) of 0.01. When the breakthrough point is reached, the protection time is called effective protection time, named as $t_{b(1\ \%)}$. The corresponding adsorption capacity is called the effective adsorption capacity q_b. q_b can be calculated from eq 2.

$$q_b = \frac{c_0 \cdot t_{b(1\ \%)} \cdot Q}{V} \quad (2)$$

where q_b is the breakthrough adsorption capacity in $mg \cdot cm^{-3}$; Q is the volumetric flow rate in $L \cdot min^{-1}$; V is the activated carbon fill volume in cm^3; and $t_{b(1\ \%)}$ is the effective protection time in min.

The regression equations and the coefficient of correlation under each airflow humidity condition for the untreated activated carbon bed are listed in Table 3.

As shown in Table 3, the coefficient of determination for the regression equations ranged between 0.9886 and 0.9980, indicating a very high degree of confidence that the straight line equations accurately represented the data.

It can be seen from Table 4 that under the same experimental conditions (inlet gas concentration, airflow rate, fill volume, and temperature), the effective adsorption capacity q_b and effective protection time t_b of the carbon bed to PFIB decreased notably

Table 3. Regression Equations for Untreated Activated Carbon Bed

airflow humidity (%)	regression equations	coefficient of determination R^2
30	$t_b = -107.57 \ln(c_0/c_x) + 945.61$	0.9910
40	$t_b = -112.80 \ln(c_0/c_x) + 935.22$	0.9980
50	$t_b = -113.30 \ln(c_0/c_x) + 914.12$	0.9886
60	$t_b = -115.75 \ln(c_0/c_x) + 877.47$	0.9948
80	$t_b = -119.42 \ln(c_0/c_x) + 857.46$	0.9912

Table 4. Calculated Results of Some Parameters for the Untreated Sample

air flow humidity (%)	effective protection time t_b/min	equilibrium adsorption capacity q_e/mg·cm^{-3}	effective adsorption capacity q_b/mg·cm^{-3}	adsorption rate constant k_v/min^{-1}
30	448	472.8	224.0	1098.8
40	402	467.6	201.0	1041.9
50	378	457.1	189.0	1008.5
60	330	438.7	165.0	947.6
80	292	428.7	154.0	897.5

Table 5. Protection Properties to PFIB in 80 % Airflow Humidity for Modified Samples

sample	effective protection time t_b/min	equilibrium adsorption capacity q_e/mg·cm^{-3}	effective adsorption capacity q_b/mg·cm^{-3}	adsorption rate constant k_v/min^{-1}
untreated	292	428.7	154.0	897.5
M-60	356	442.2	178.0	994.2
M-120	404	468.6	202.0	1047.9
M-180	426	454.4	213.0	1078.4

with an increase of airflow humidity. As the airflow humidity rose from 30 % to 80 %, the effective protection time t_b depressed from (448 to 292) min decreased by 34.8 %. The effective adsorption capacity, depressed from 224 mg·cm^{-3} to 154 mg·cm^{-3}, decreased by 31.3 %. At the same time, both the equilibrium adsorption capacity q_e and the adsorption rate constant k_v decreased. Because of the effect of competitive adsorption of water molecules, the adsorption rate of the carbon bed to PFIB depressed, the bed availability decreased.

The activated carbon surface is hydrophilic because of a great deal of oxygen-containing groups. The water molecules adsorbed competitively on the carbon surface with PFIB vapor, taking the pore space, thus making the effective adsorption capacity of the carbon bed to PFIB much less. The effect of water molecules became greater with the increase of airflow humidity. Microwave modification can diminish the surface oxygen-containing groups and then enhance the hydrophobicity of the carbon surface, so the competition effect of water molecules in the airflow decreased, especially in high humidity conditions. Table 5 shows the protection properties of microwave modified carbons against PFIB in an 80 % airflow humidity condition.

As shown in Table 5, the effective protection time t_b and effective adsorption capacity q_b of modified carbons against PFIB increased notably after microwave modifications. Based on the untreated carbon's protection property, the effective protection time t_b of the M-120 sample prolonged from (292 to 426) min increased by 45.9 %. The effective adsorption capacity q_b of the M-120 sample rose from 154 mg·cm^{-3} to 213 mg·cm^{-3} and increased by 38.3 %. In addition, the equilibrium adsorption capacity q_e and adsorption rate constant k_v increased greatly, meaning that the bed height of adsorption saturation decreased and the bed availability was depressed.

We have discussed in Table 1 that the S_{BET} and pore structure of modified carbons did not change much after microwave modifications, so the increase of the protection property should attribute to the removal of oxygen-containing groups on the carbon surface.

Adsorption Kinetics Fitting. The Wheeler equation is only suitable for low concentration penetration points, so an additional model which can predict the entire breakthrough curve is necessary. To develop a mathematical model to analyze the experimental results and fixed bed dynamics, the following approximations are assumed.

(1) The adsorption process is isothermal;

(2) Axial dispersion is neglected;

(3) The equilibrium relationship for the adsorbing component is represented by the Langmuir isotherm;

(4) The mass transfer rate is represented by a linear driving force rate expression;

(5) The ideal gas law applies.

The adsorption isotherms of most single-component systems in low concentration are linear (the Langmuir adsorption isotherm at the low concentration zone can be assumed to be a straight line). Based on the linear driving force (LDF) model, the component mass balance equation, mass transfer equation, and adsorption isotherm equation were combined and solved by parameter transformation and Laplace transform to get the relationship between the exit concentration and time, and the theoretical breakthrough curve can be written as

$$\frac{c}{c_0} = e^{-X-T} I_0(2\sqrt{XT}) + \int_0^T e^{-X-T} I_0(2\sqrt{XT}) dT \qquad (3)$$

where I_0 is a zero-order Bessel function, expressed by eq 4.

$$I_0(x) = \sum_{k=0}^{\infty} \frac{2}{k!\,\Gamma(k+1)} \left(\frac{x}{2}\right)^{2k} \qquad (4)$$

The approximate solution can be obtained by the error function

$$\frac{c}{c_0} = \frac{1}{2}[1 + erf(E)] \qquad (5)$$

$$E = \frac{T - X}{2\sqrt{X}} \qquad (6)$$

where $X = K_F a_v Z/uT = K_F a_v t/K_H \rho_b$; u is the linear velocity in cm·min^{-1}; ρ_b is the bulk density of packed bed in mg·cm^{-3}; Z is the bed length in cm; t is the time in min; $k_F a_v$ is the overall mass transfer coefficient in min^{-1}; and K_H is the Henry's law constant in min^{-1}.

Based on the experimental data, E can be calculated by eq 5, and then the relationship between E and t was fitted via eq 6. In this study, the theoretical breakthrough equations of untreated carbon and the M-180 sample at 30 % and 80 % airflow humidity were obtained by linear regression, respectively.

As shown in Figure 4, the regression curves of $E \sim t$ under various conditions all presented considerable linearity, and the lowest coefficient of determination reaches 0.9889. Each theoretical breakthrough equation and calculated $K_F a_v$ values were shown in Table 6.

For the untreated carbon, the overall mass transfer coefficient $K_F a_v$ decreased by 27.3 % from 30 % humidity to 80 % humidity, which indicated that the mass transfer resistance caused by the water molecules increased and the effective adsorption capacity of PFIB decreased greatly. The $K_F a_v$ of M-180 to PFIB increased just a little more than that of untreated carbon at 30 % airflow humidity, indicating that modification had little effect on the adsorption to PFIB at low airflow humidity. However, the $K_F a_v$ of M-180 to PFIB increased greatly compared to that of untreated carbon at 80 % airflow

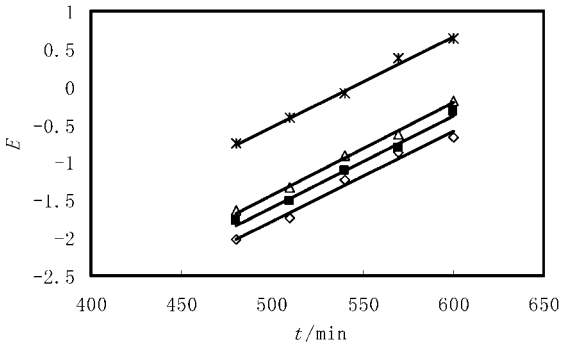

Figure 4. Regression curves between E and t: ■, untreated-30 %; ◇, modified-30 %; *, untreated-80 %; △, modified-80 %.

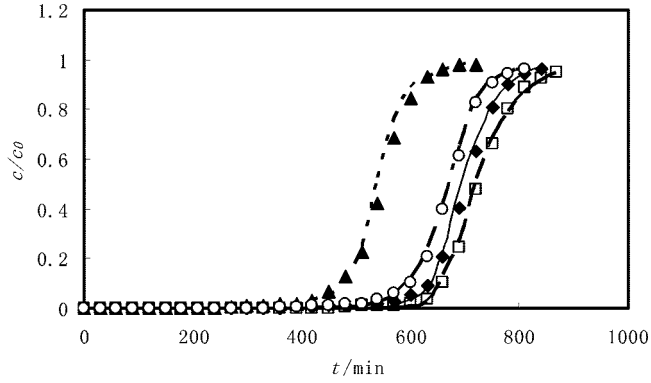

Figure 5. Comparison of theoretical curves and experimental data: ♦, untreated-30 %-E; —, untreated-30 %-T; □, modified-30 %-E; — —, modified-30 %-T; ▲, untreated-80 %-E; ----, untreated-80 %-T; ○, modified-80 %-E; — - —, modified-80 %-T. (E-Experimental; T-Theoretical; Inlet concentration, 4 mg·L^{-1}; experiment temperature, 25 °C).

Table 6. Theoretical Breakthrough Curves and Calculated $K_F a_v$ Value

sample	theoretical breakthrough equation	coefficient of determination R^2	calcd $K_F a_v$ min^{-1}
untreated-30 %	$c/c_0 = 0.5[1 + erf(0.0121t - 7.626)]$	0.9889	29077
M-180-30 %	$c/c_0 = 0.5[1 + erf(0.0119t - 7.752)]$	0.9949	30046
untreated-80 %	$c/c_0 = 0.5[1 + erf(0.0119t - 6.503)]$	0.9951	21144
M-180-80 %	$c/c_0 = 0.5[1 + erf(0.0121t - 7.492)]$	0.9959	28065

humidity and even approached the $K_F a_v$ value of untreated carbon at 30 % airflow humidity. So, it is concluded that the microwave modification decreased the competitive adsorption notably, especially in high airflow humidity, and enhanced the adsorption property of PFIB greatly. Figure 5 shows the theoretical curves and the corresponding experimental data of untreated carbon and M-120 carbon under 30 % and 80 % airflow humidity, respectively.

As shown in Figure 5, the theoretical curves under low airflow humidity (30 %) and high airflow humidity (80 %) agreed well with their experimental data. So it is feasible to apply the model based on the linear driving force (LDF) system to predict the breakthrough behavior of PFIB on the activated carbon, thus providing the parameter design of the respirator cartridge with reliable data.

Conclusions

(1) The air humidity has a considerable effect on the adsorption capacity of PFIB on the activated carbon bed. The adsorption rate constant of PFIB decreased with the increase of airflow humidity due to the competitive adsorption of water molecules. At the same time, the effective adsorption capacity and effective protection time decreased, indicating the bed availability was depressed.

(2) The pore structure of the activated carbon did not change obviously after microwave modification, whereas the surface oxygen content decreased greatly and the surface became more hydrophobic. The competitive adsorption of water molecules decreased greatly, and the effective protection time was prolonged, especially at high airflow humidity (80 %).

(3) Based on the linear driving force (LDF) model, the approximate solution of the piston flow fixed bed theoretical breakthrough curve was used to simulate the breakthrough behavior. The results showed that the theoretical breakthrough curves agreed well with the experimental data, so it is practical to predict the breakthrough behavior of PFIB on the activated carbon bed and also to choose the respirator cartridge parameters with this model.

Literature Cited

(1) Vahdat, N. Theoretical study of the performance of activated carbon in the presence of binary vapor mixtures. *Carbon* **1997**, *35* (10−11), 1545–1557.
(2) Wood, G. O.; Stampfer, J. F. Adsorption rate coefficients for gases and vapors on activated carbons. *Carbon* **1993**, *31* (1), 195–200.
(3) Lailey, A. F.; Hill, L.; Lawston, I. W.; Stanton, D.; Upshall, D. G. Protection by cysteine esters against chemically induced pulmonary oedema. *Biochem. Pharmacol.* **1991**, *42*, 47–54.
(4) Arroyo, C. M. The chemistry of perfluoroisobutylene (PFIB) with nitrone and nitroso spin traps: an EPR/Spin trapping study. *Chem.-Biol. Interact.* **1997**, *105*, 119–129.
(5) Oberdorster, G.; Ferin, J.; Gelein, R.; Finkelstein, J.; Baggs, R. Effects of PTFE fumes in the respiratory tract: a particle effect. *Aerospace Medical Association 65th Annual Scientific Meeting,* **1994**, *538*, A52.
(6) Zhang, H.; Cheng, D. Mathematical model for a fixed bed adsorptive reactor. *Carbon* **2000**, *38*, 877–880.
(7) Chuang, C.L.; Chian, P. C.; Chang, E. E. Modeling VOCs adsorption onto activated carbon. *Chemosphere* **2003**, *53*, 17–27.
(8) Wang, K.; Qiao, S.; Hu, X. Study of isosteric heat of adsorption and activation energy for surface diffusion of gases on activated carbon using equilibrium and kinetics information. *J. Hazard. Mater.* **2004**, *34*, 165–176.
(9) Liu, H.; Lu, G.; Guo, Y.; Guo, Y.; Wang, J. Chemical kinetics of hydroxylation of phenol catalyzed by TS-1/diatomite in fixed-bed reactor. *J. Chem. Eng.* **2006**, *116*, 179–186.
(10) Hameed, B. H.; Din, A. T. M.; Ahmad, A. L. Adsorption of methylene blue onto bamboo-based activated carbon: Kinetics and equilibrium studies. *J. Hazard. Mater.* **2007**, *141*, 819–825.
(11) Jonas, L. A.; Rehrmann, J. A. Predictive equations in gas adsorption kinetics. *Carbon* **1973**, *11*, 59–64.

Received for review October 31, 2007. Accepted March 20, 2008.

JE7006346